Supplementary Information and Figures

New Ruthenium(II) Complexes with Enantiomerically Pure Bis- and Tris(pinene)-Fused tridentate ligands. Synthesis, characterization and Stereoisomeric Analysis

Xavier Sala, Isabel Romero, Montserrat Rodríguez, Albert Poater, Antoni Llobet*, Alexander von Zelewsky, Teodor Parella, Xavier Fontrodona, Miquel Solà*.*

Figure S1. X-ray structure and labeling scheme for the cationic part of complex **8a**. Hydrogen bonding interaction.

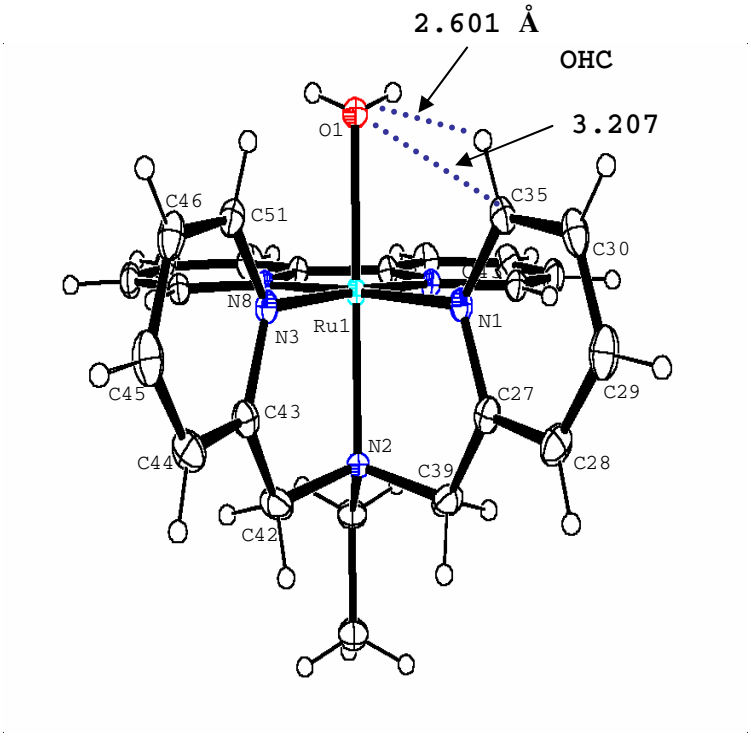

Table S1. Geometrical comparison between the X-ray data of isomer **4a** and the corresponding B3PW91 geometry (Distances in Å and angles in degrees).

Distances	dist(RX)	dist(B3LYP)	Angles	ang(RX)	ang(B3LYP)
Ru-N1	2.222	2.227	N3-Ru-N2	77.6	78.4
Ru-N2	2.173	2.187	N3-Ru-N1	81.0	79.7
Ru-N3	2.246	2.283	N2-Ru-N1	81.2	80.8
Ru-Cl1	2.454	2.448	N3-Ru-P1	176.3	176.5
Ru-P1	2.307	2.331	N2-Ru-P1	100.1	99.5
Ru-P2	2.320	2.351	N1-Ru-P1	95.8	97.2
P1-C13	1.850	1.864	N1-Ru-P2	178.4	177.4
P2-C14	1.847	1.860	N3-C43-C42	117.2	117.2
C13-C14	1.534	1.525	N2-Ru-P2	98.8	97.6
N2-C39	1.489	1.485	P1-Ru-P2	85.8	85.1
N2-C42	1.484	1.481	N3-Ru-Cl1	97.1	97.9
C39-C27	1.498	1.502	N1-Ru-Cl1	100.8	102.2
C42-C43	1.500	1.493	N2-Ru-Cl1	174.1	174.8
N1-Cl	3.642	3.604	P1-Ru-Cl1	85.3	84.4
N3-Cl	3.547	3.548	P2-Ru-Cl1	79.1	79.2
P1-C1	1.834	1.849	P1-C13-C14	111.1	110.4
P1-C7	1.852	1.859	P2-C14-C13	111.7	111.2
P2-C21	1.842	1.861	N2-C39-C27	115.8	114.8
P2-C15	1.837	1.844	N2-C42-C43	113.1	112.8
N2-C40	1.503	1.500	C1-P1-C7	99.2	99.5
C40-C41	1.532	1.528	C15-P2-C21	97.7	97.6

Figure S2. Relative energy diagram for the BP3W91-optimized geometries of the cationic moieties of complexes **8a**-**8d.**

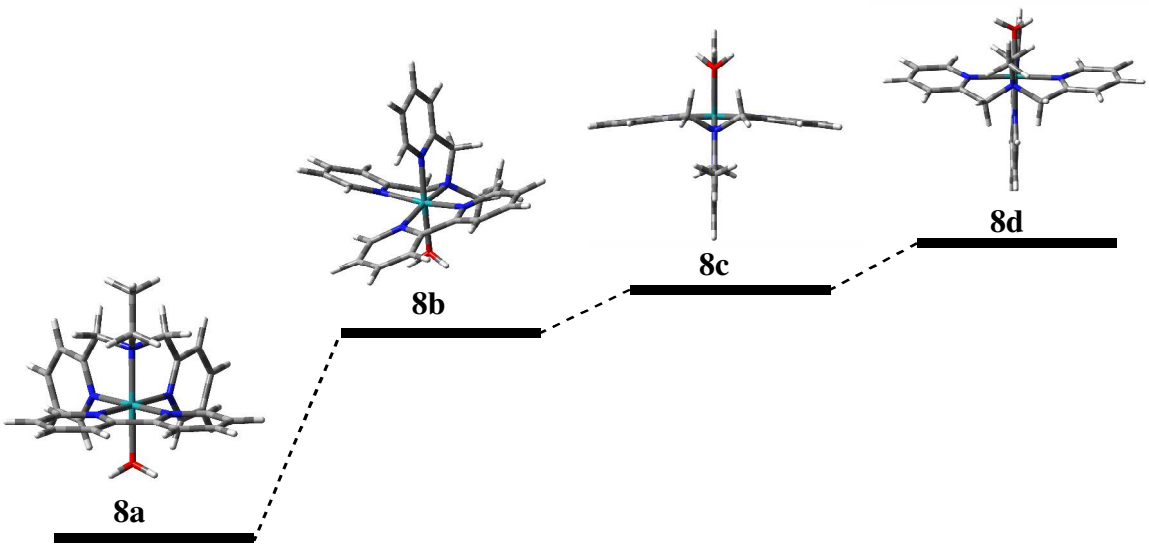

Figure S3. NMR (500 MHz, 298 K, CD_2Cl_2) spectra for complex **3a**: (a) 1H-NMR, (b) 13C-NMR, (c) NOESY (d) HMBC (e) HSQC.

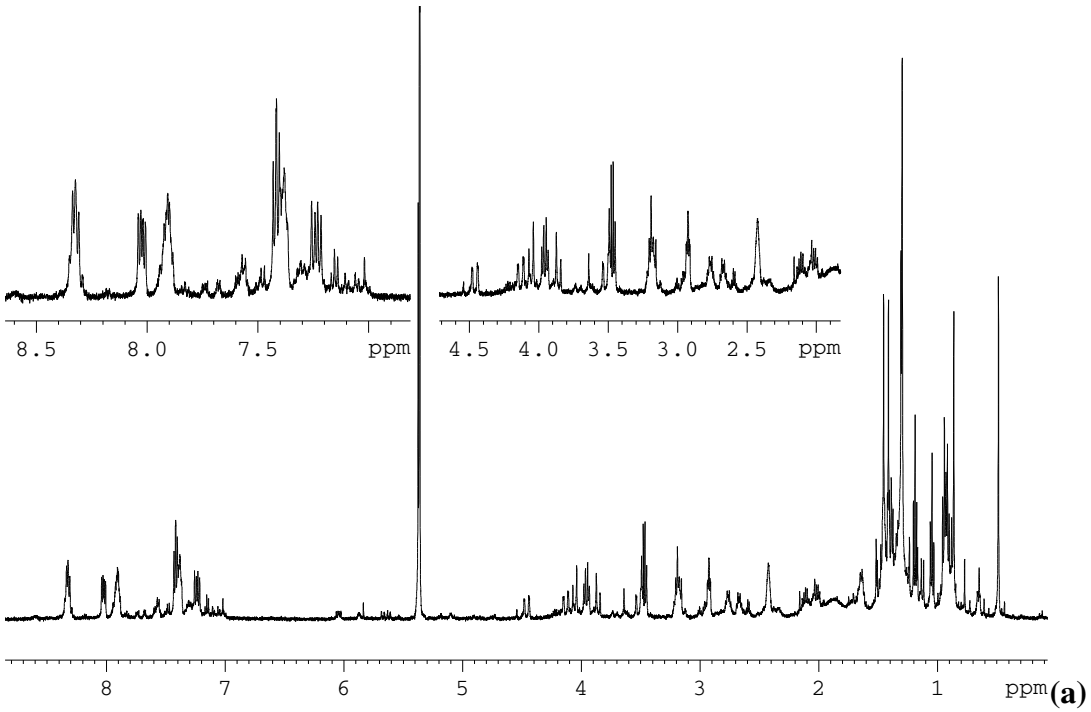

(a)

(b)

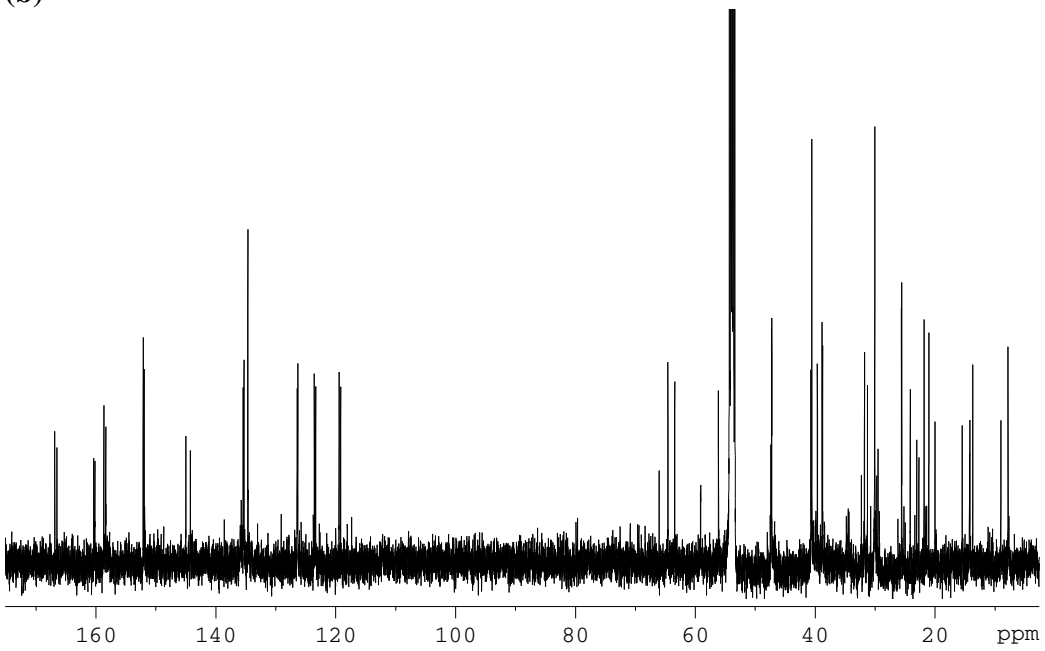

(c)

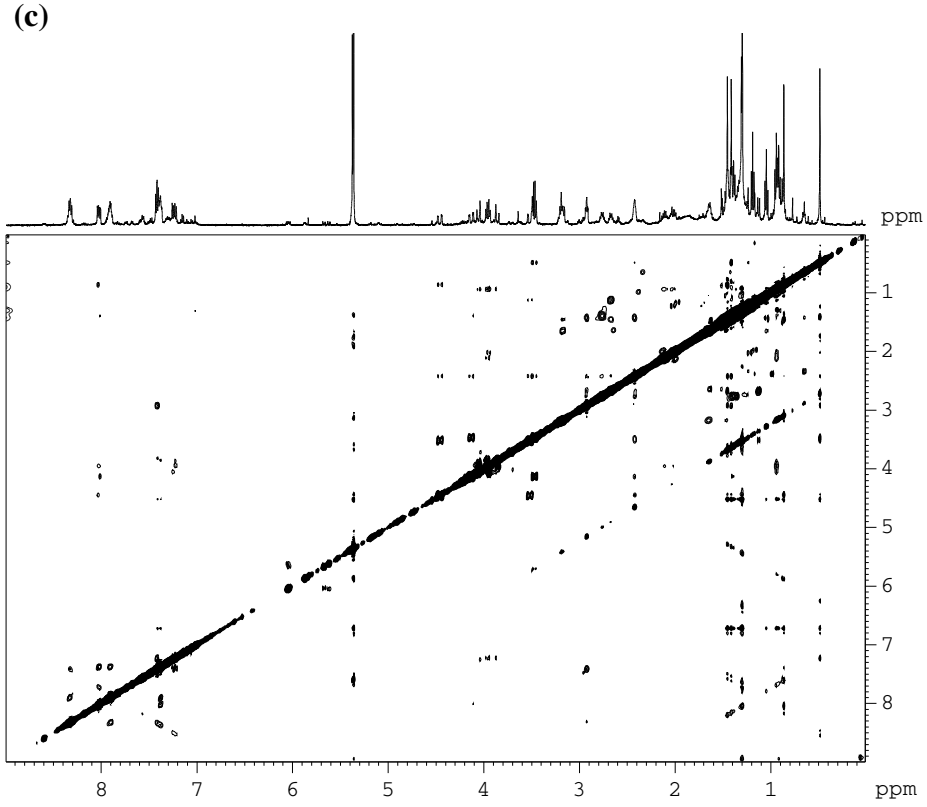
ppm
1
2
3
4
5
6
7
8
8
7
6
5
4
3
2
1
ppm

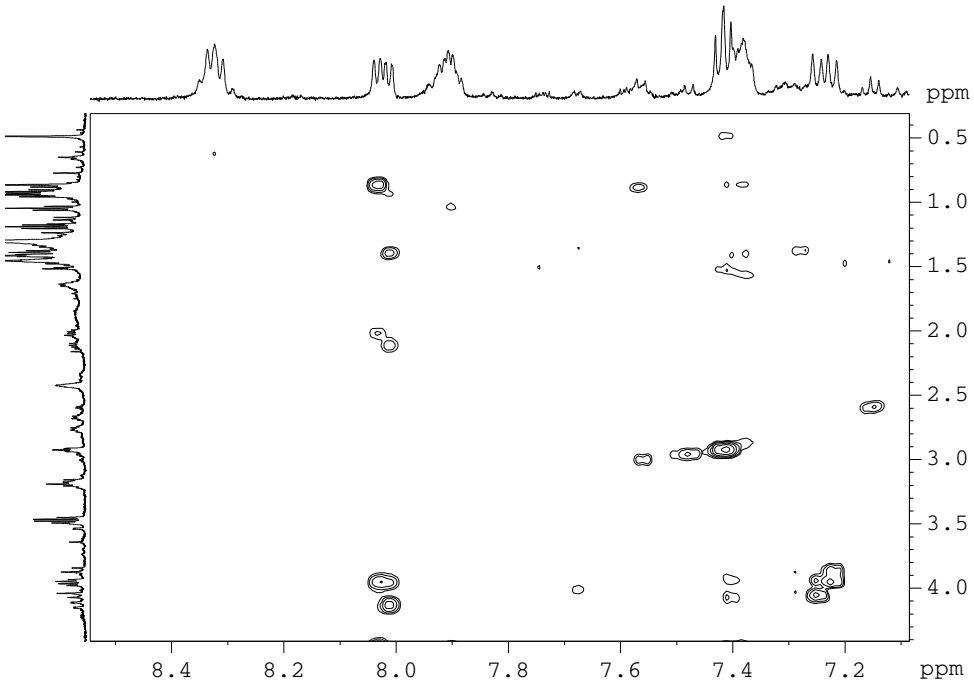
ppm
0.5
1.0
1.5
2.0
2.5
3.0
3.5
4.0
8.4
8.2
8.0
7.8
7.6
7.4
7.2
ppm

(d)

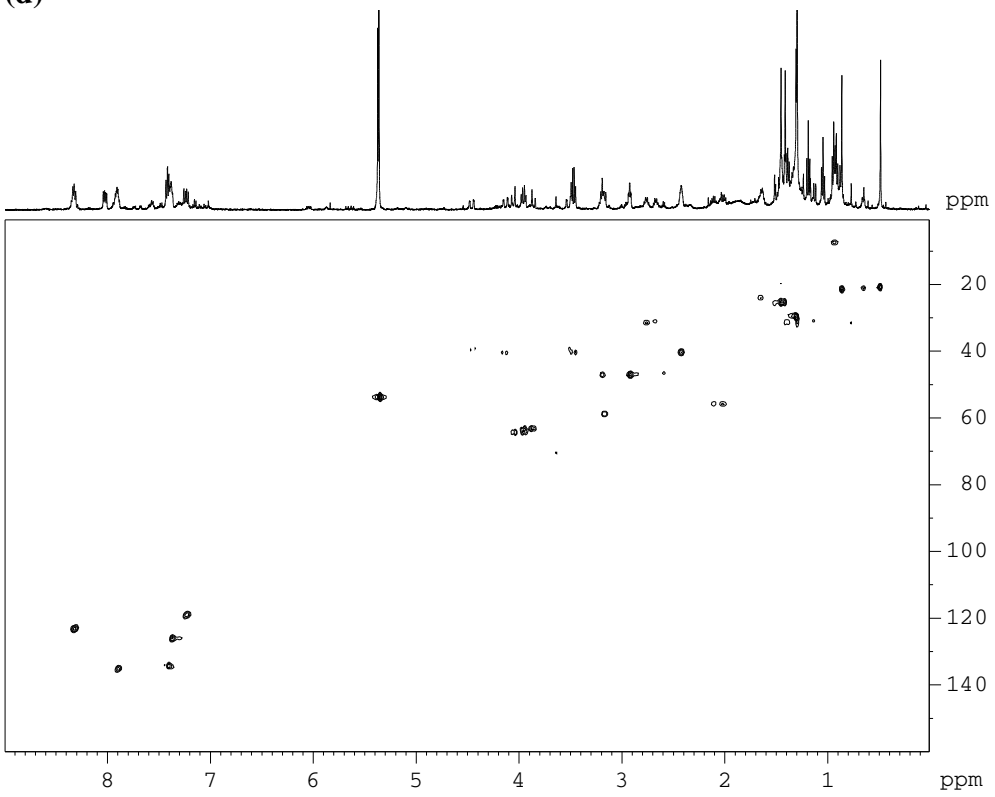
ppm
20
40
60
80
100
120
140
8
7
6
5
4
3
2
1
ppm

(e)

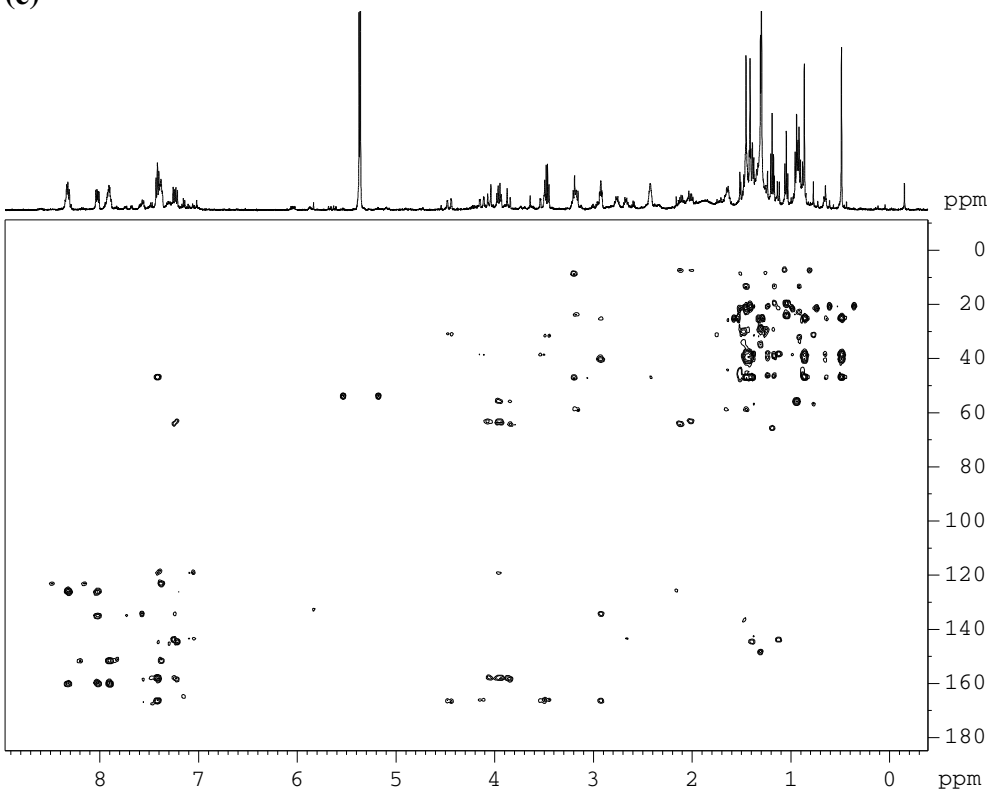
ppm
0
20
40
60
80
100
120
140
160
180
8
7
6
5
4
3
2
1
0
ppm

Figure S4. NMR (500 MHz, 298 K, CD_2Cl_2) spectra for complex **4a**: (a) 1H-NMR, (b)31P-NMR, (c) NOESY (d) HMBC (e) HSQC (f) HMBC 1H-31P

(a)

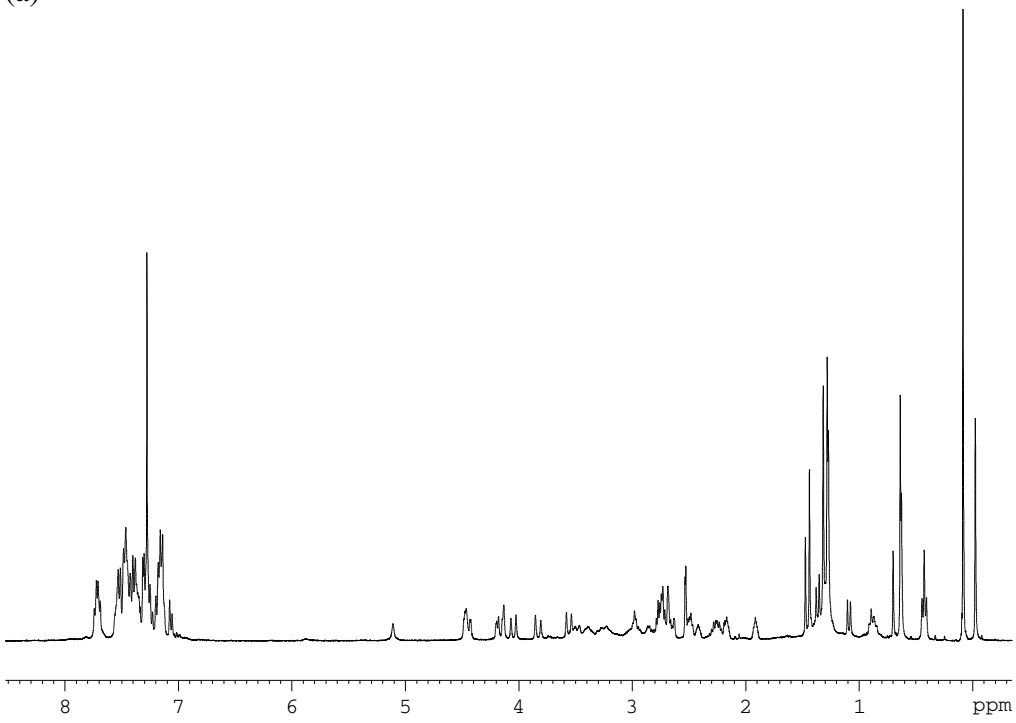

(b)

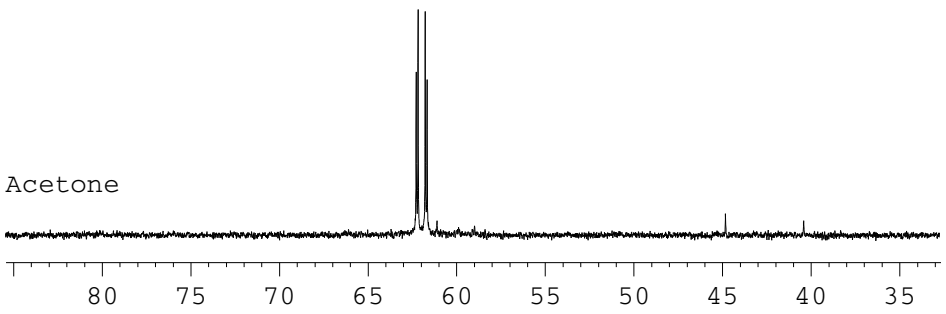

(c)

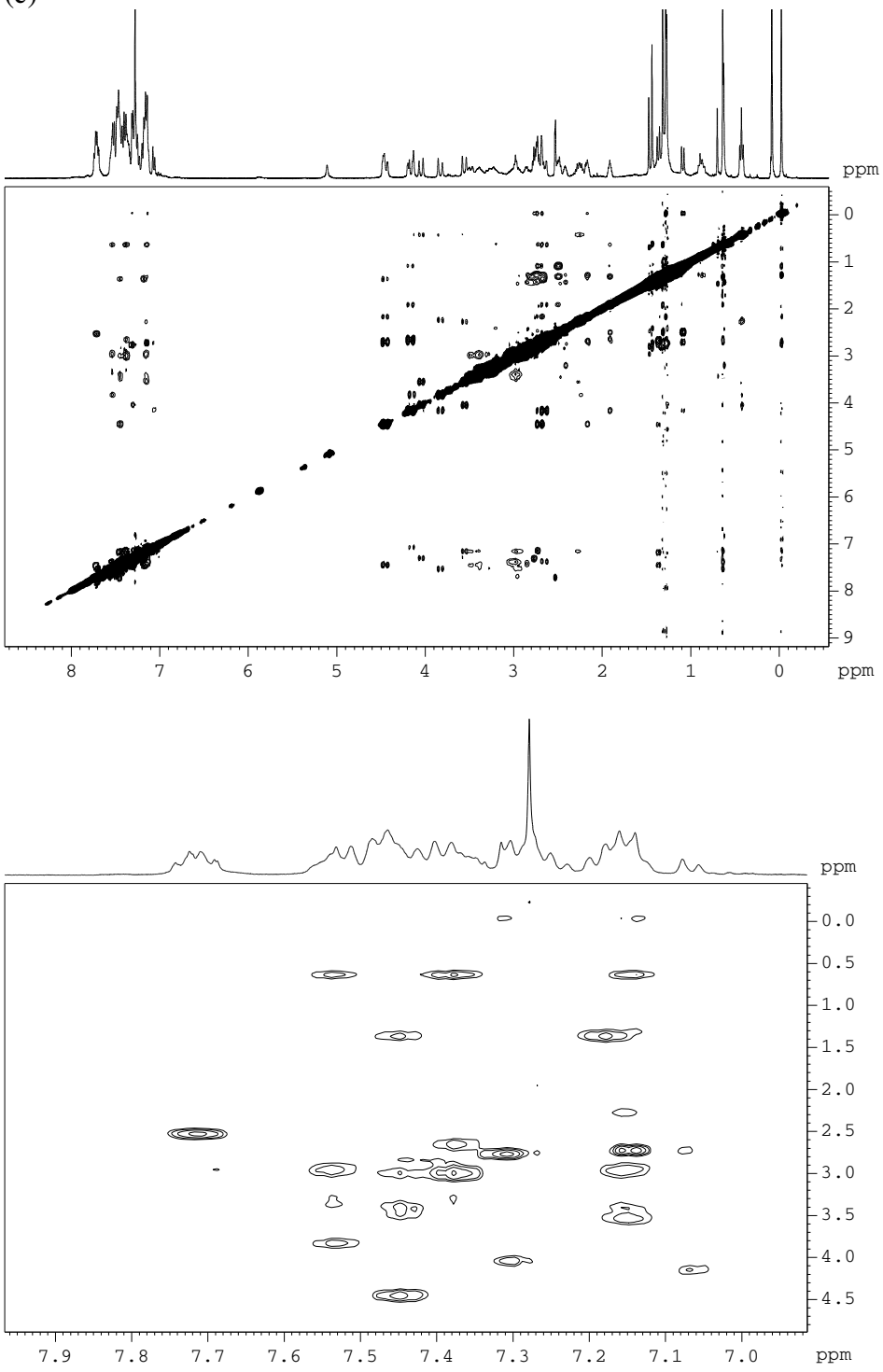
ppm
0
1
2
3
4
5
6
7
8
9
8
7
6
5
4
3
2
1
0
ppm
ppm
0.0
0.5
1.0
1.5
2.0
2.5
3.0
3.5
4.0
4.5
7.9
7.8
7.7
7.6
7.5
7.4
7.3
7.2
7.1
7.0
ppm

(d)

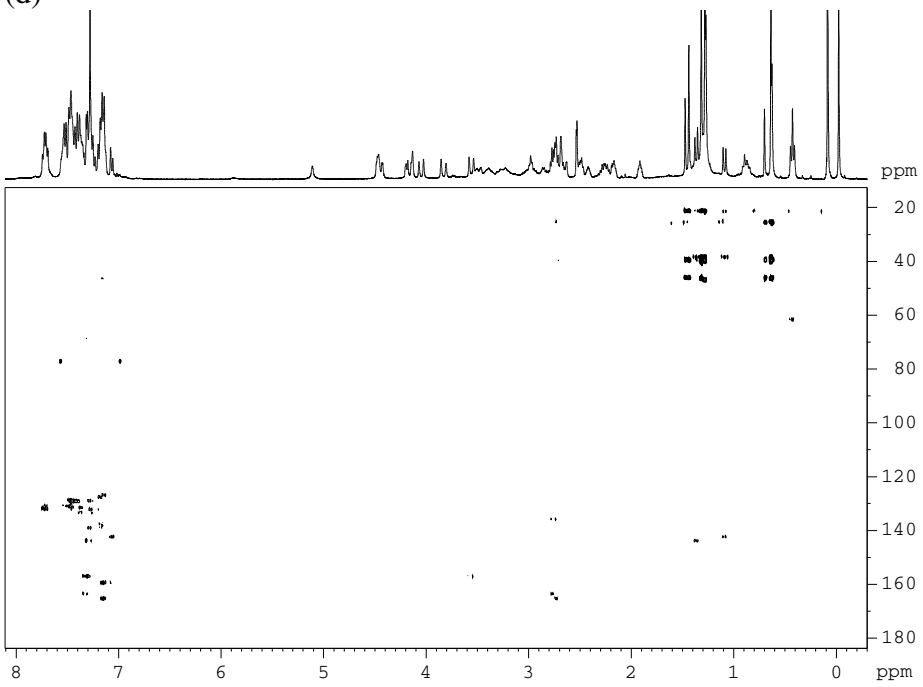
ppm
20
40
60
80
100
120
140
160
180
8
7
6
5
4
3
2
1
0
ppm

(e)

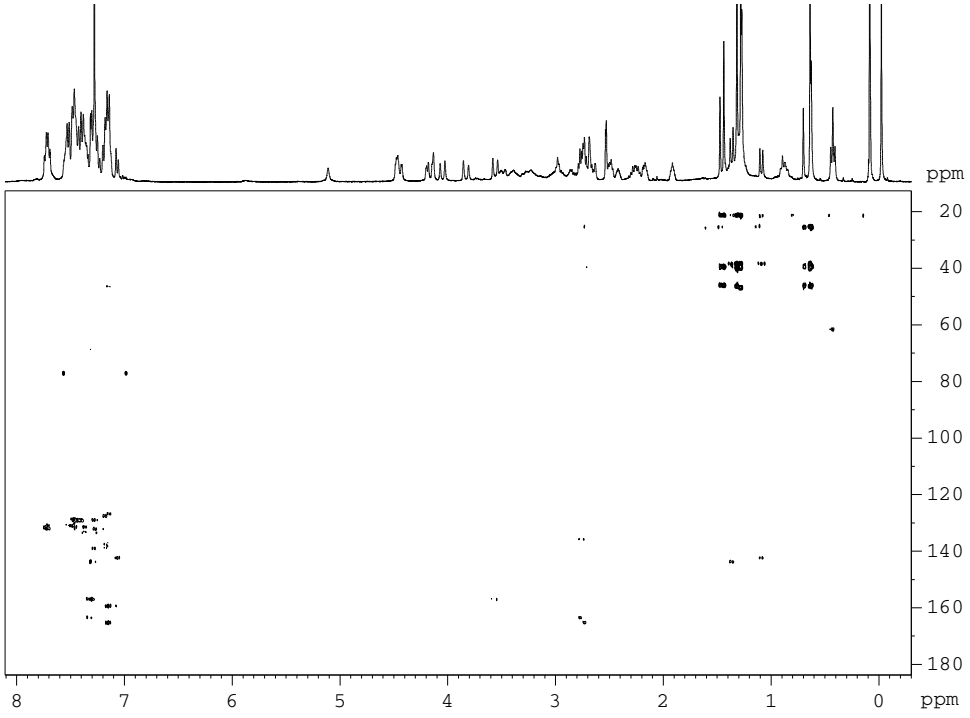
ppm
20
40
60
80
100
120
140
160
180
8
7
6
5
4
3
2
1
0
ppm

(f)

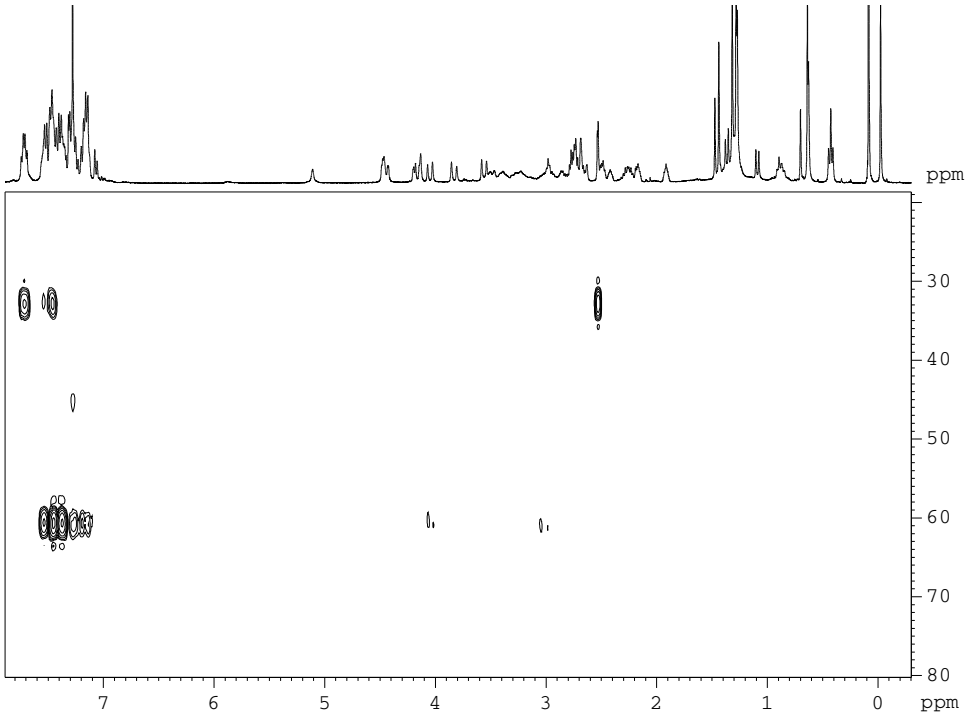

Figure S5. NMR (500 MHz, 298 K, $CDCl_3$) spectra for complex **5**: (a) 1H-NMR, (b)13C-NMR, (c) NOESY (d) HMBC (e) HSQC

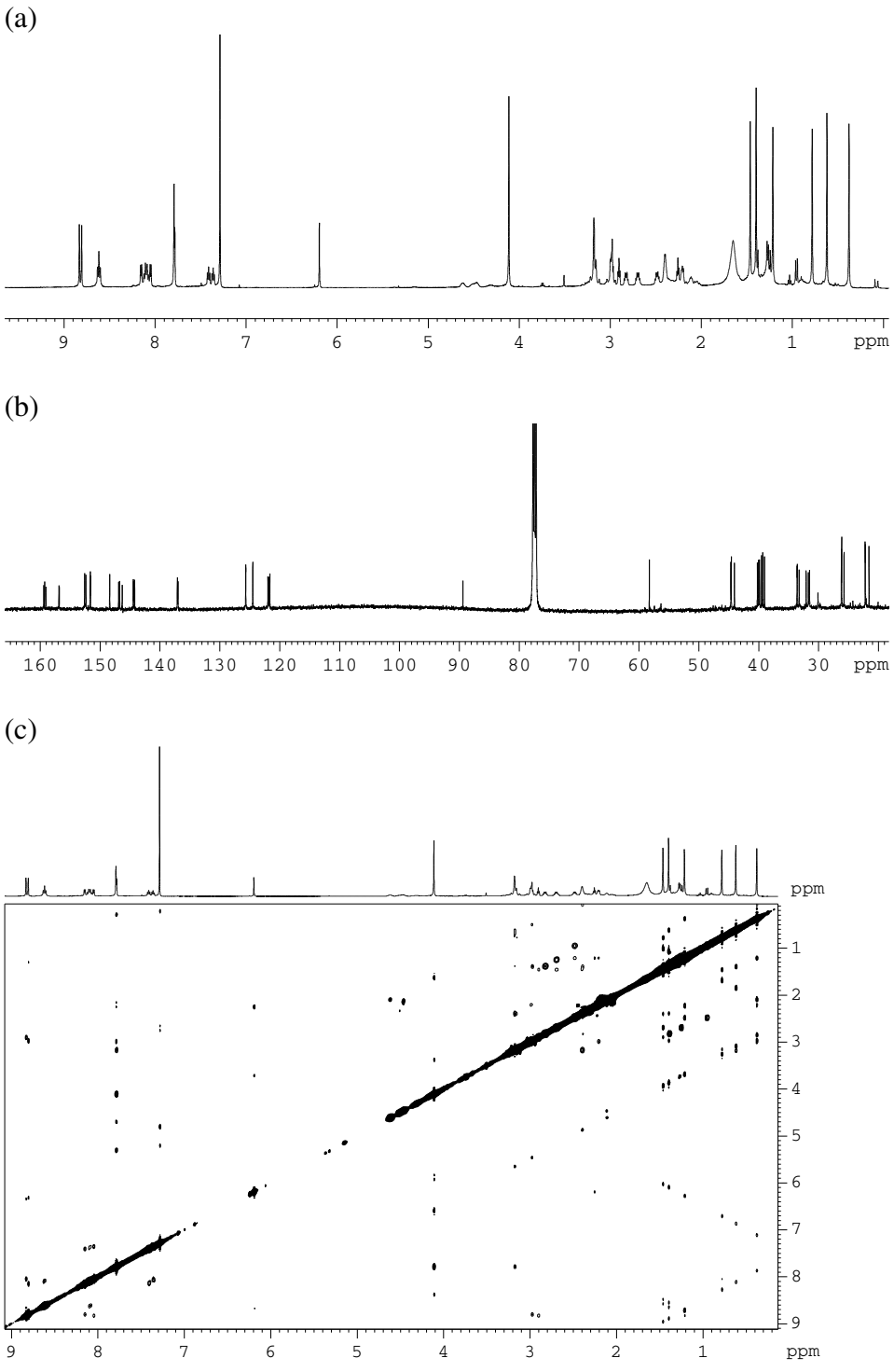

(d)

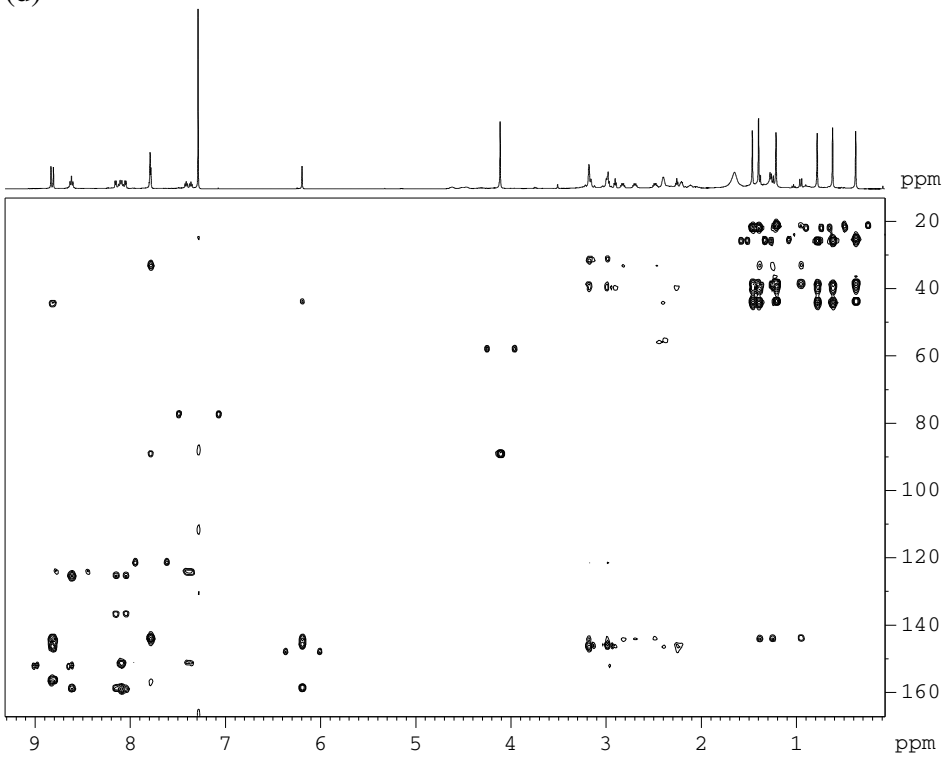
ppm
20
40
60
80
100
120
140
160
9
8
7
6
5
4
3
2
1
ppm

(e)

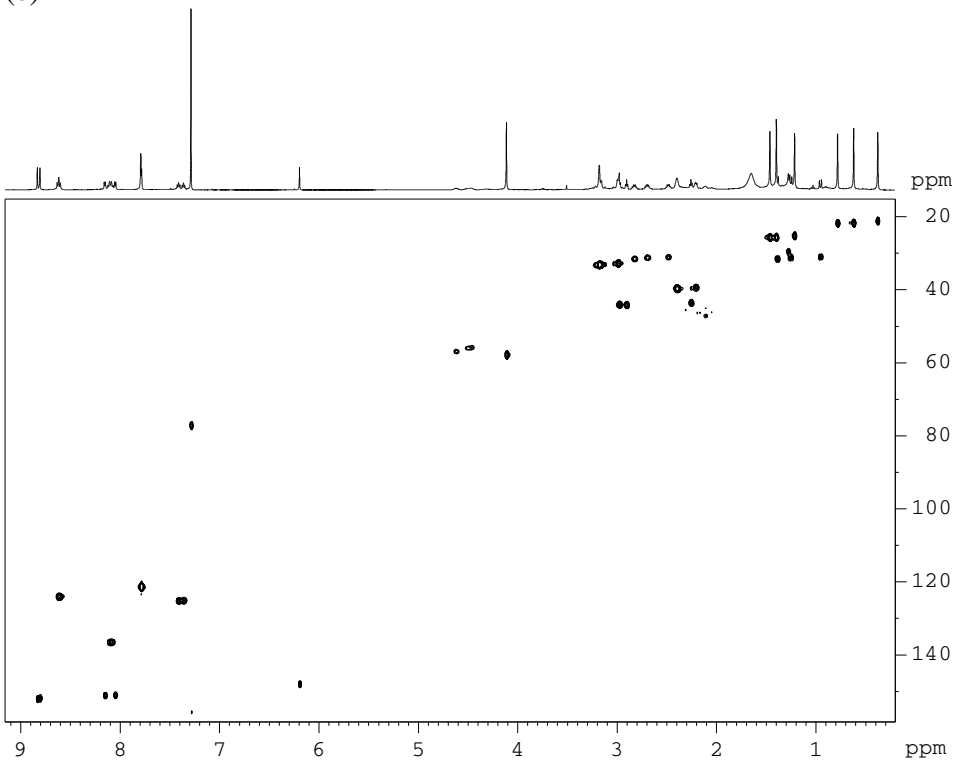
ppm
20
40
60
80
100
120
140
9
8
7
6
5
4
3
2
1
ppm

Figure S6. NMR (500 MHz, 298 K, $CDCl_3$) spectra for complex **6**: (a) 1H-NMR, (b)31P-NMR, (c) NOESY (d) HMBC (e) HSQC (f) 1H-31P HMBC

(a)

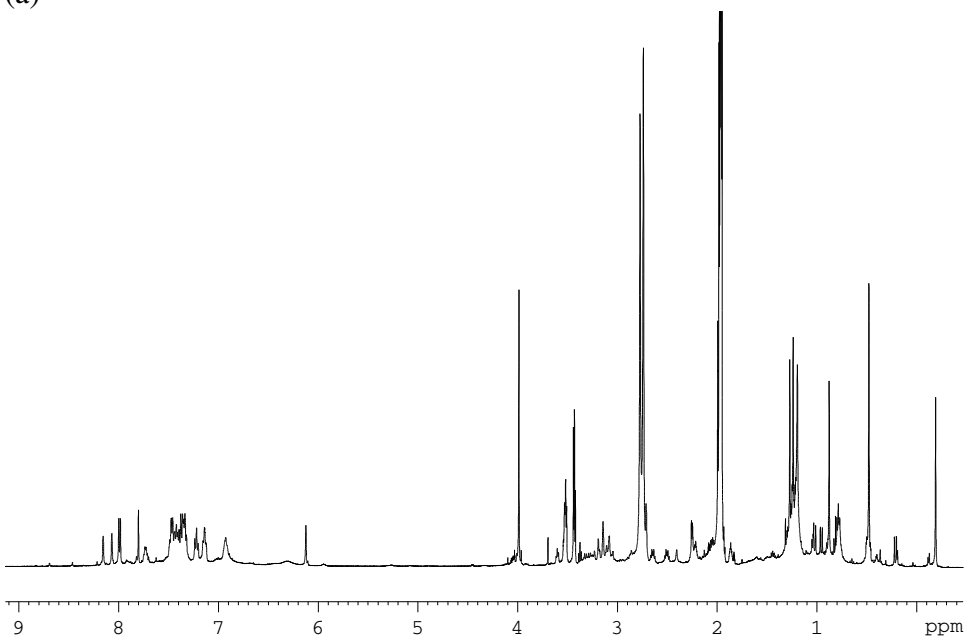

(b)

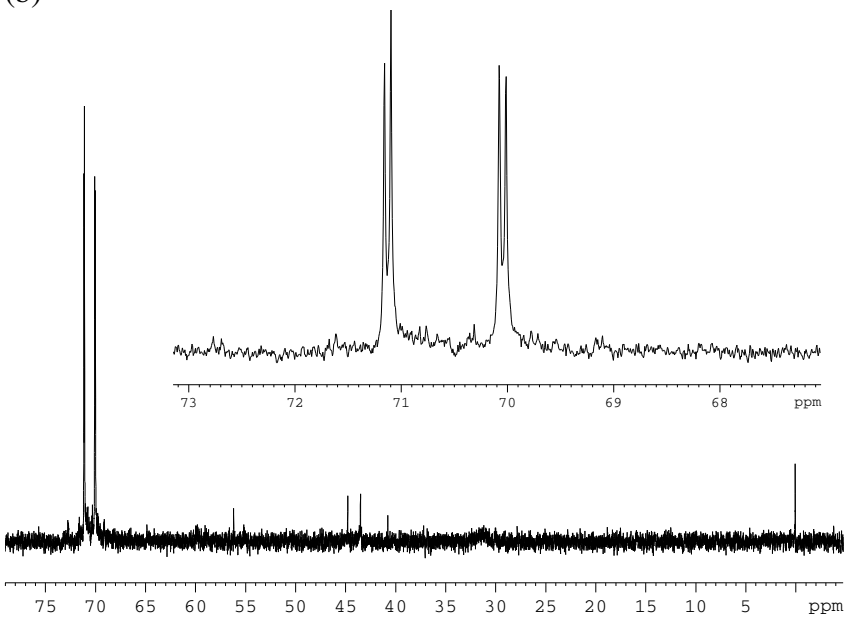

(c)

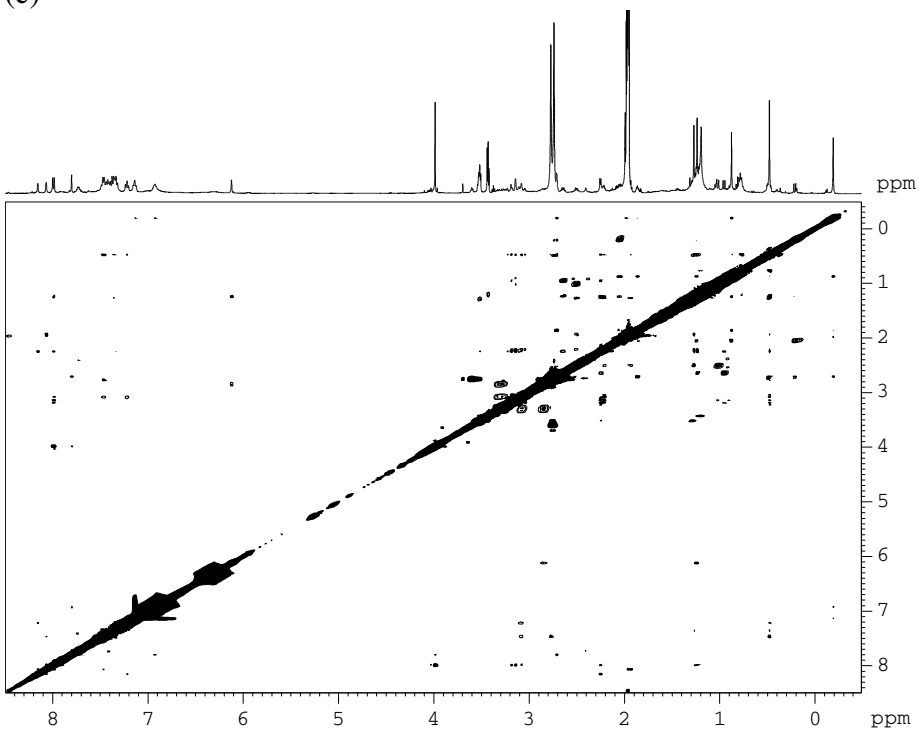
ppm
0
1
2
3
4
5
6
7
8
8
7
6
5
4
3
2
1
0
ppm

(d)

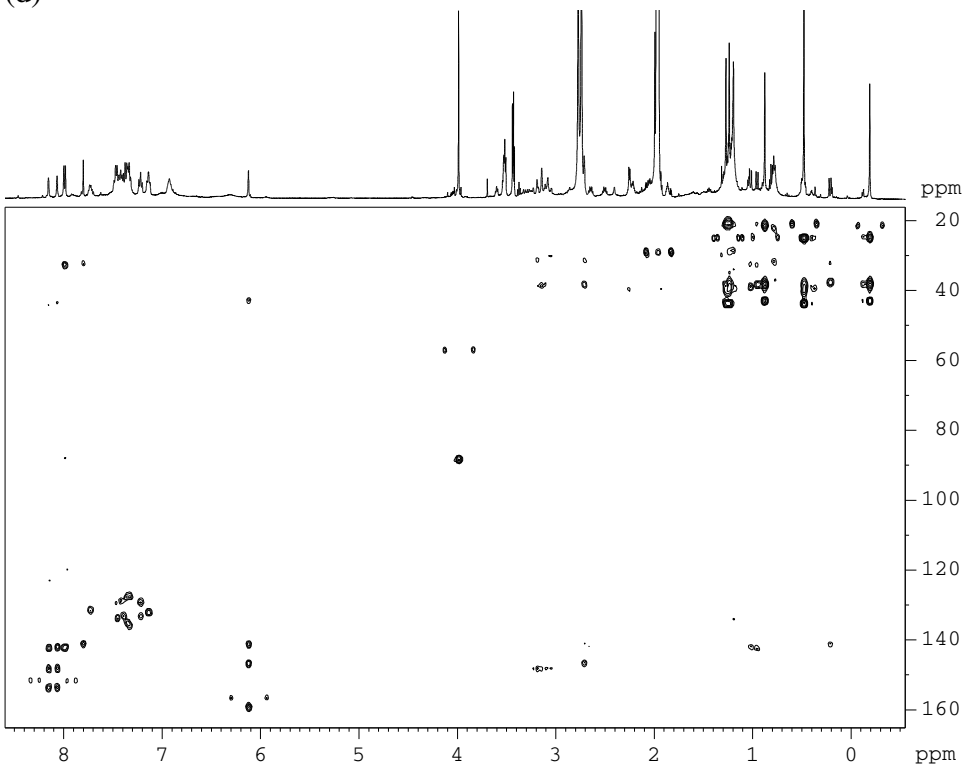
ppm
20
40
60
80
100
120
140
160
8
7
6
5
4
3
2
1
0
ppm

(e)

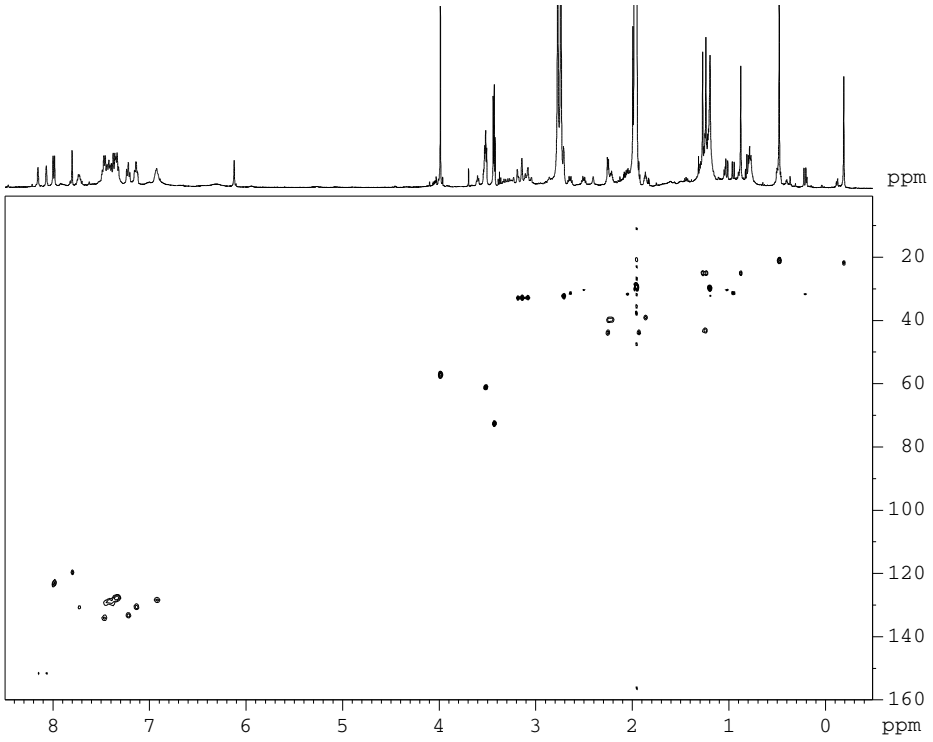
ppm
20
40
60
80
100
120
140
160
8
7
6
5
4
3
2
1
0
ppm

(f)

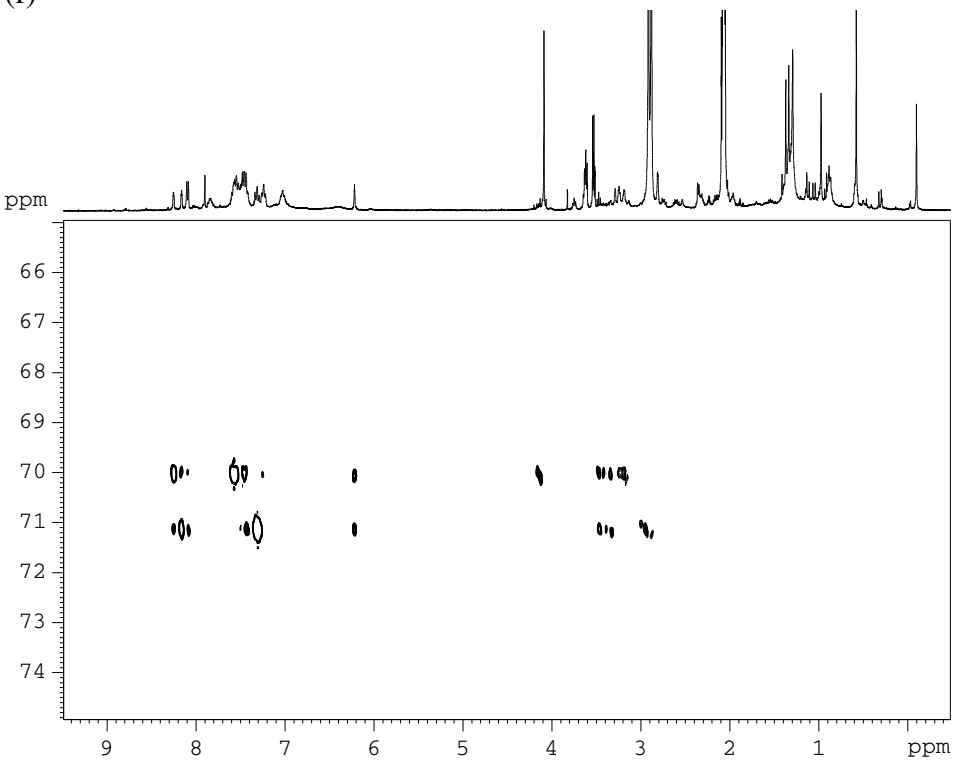
ppm
66
67
68
69
70
71
72
73
74
9
8
7
6
5
4
3
2
1
ppm

Figure S7. Cyclic Voltammetry (CH_2Cl_2 + 0,1M TBAP, 100 mV/s) of [Ru(L1 or L2)Cl_3] complexes. (a) [Ru(L1)Cl_3], **1**. (b) [Ru(L2)Cl_3], **2**.

(a)

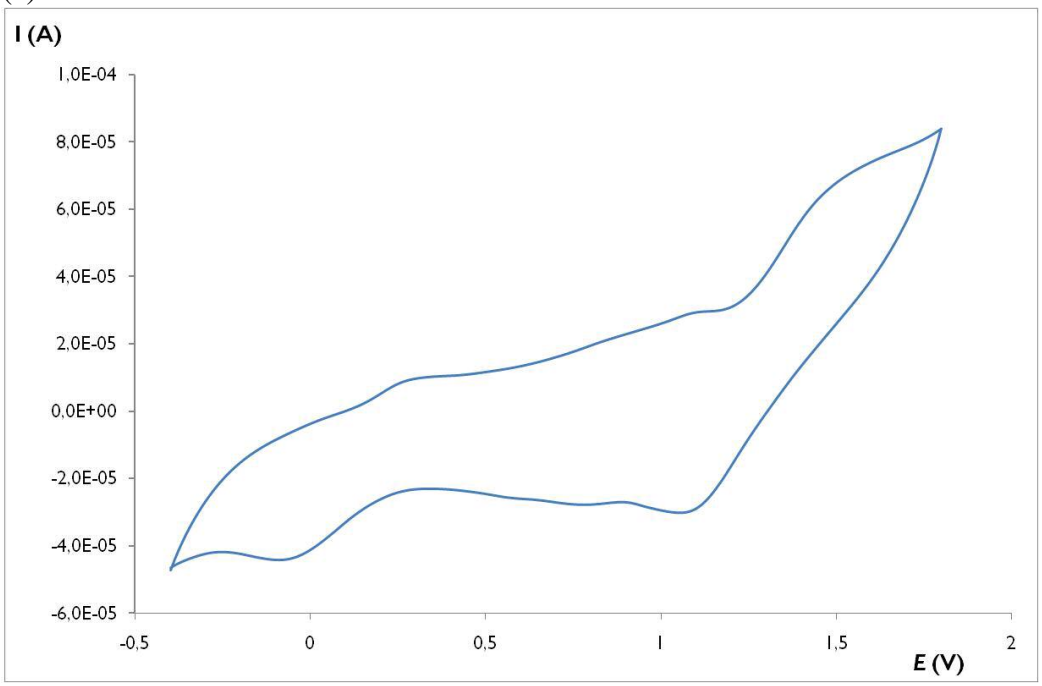

(b)

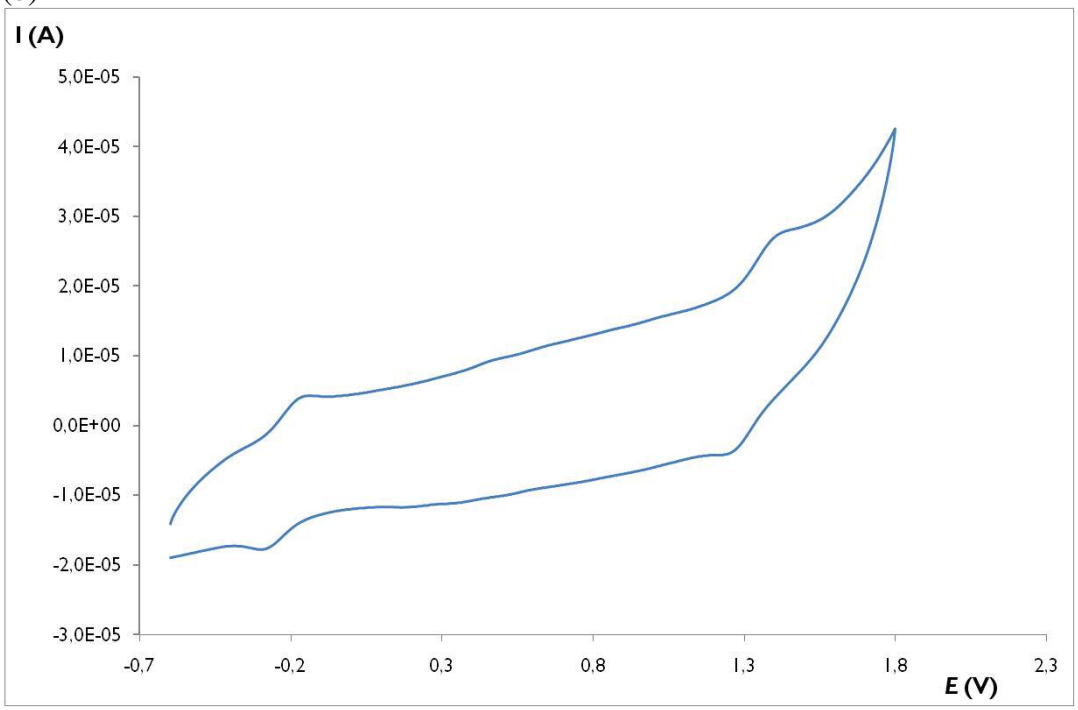

Figure S8. Cyclic Voltammetry (CH_2Cl_2 + 0,1M TBAP, 100 mV/s) of *trans,fac* complexes. (a) *trans,fac*-[Ru^{II}Cl(L1)(bpy)](BF_4)**, 3a**. (b) *trans,fac*-[Ru^{II}Cl(L1)(dppe)](BF_4)**, 4a**.

(a)

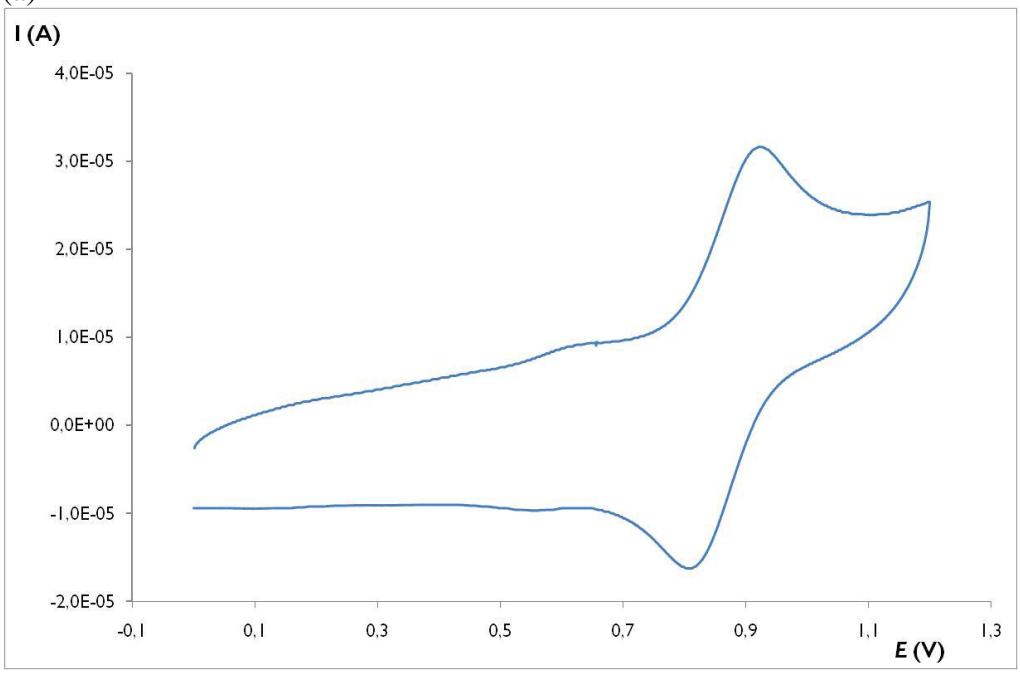

(b)

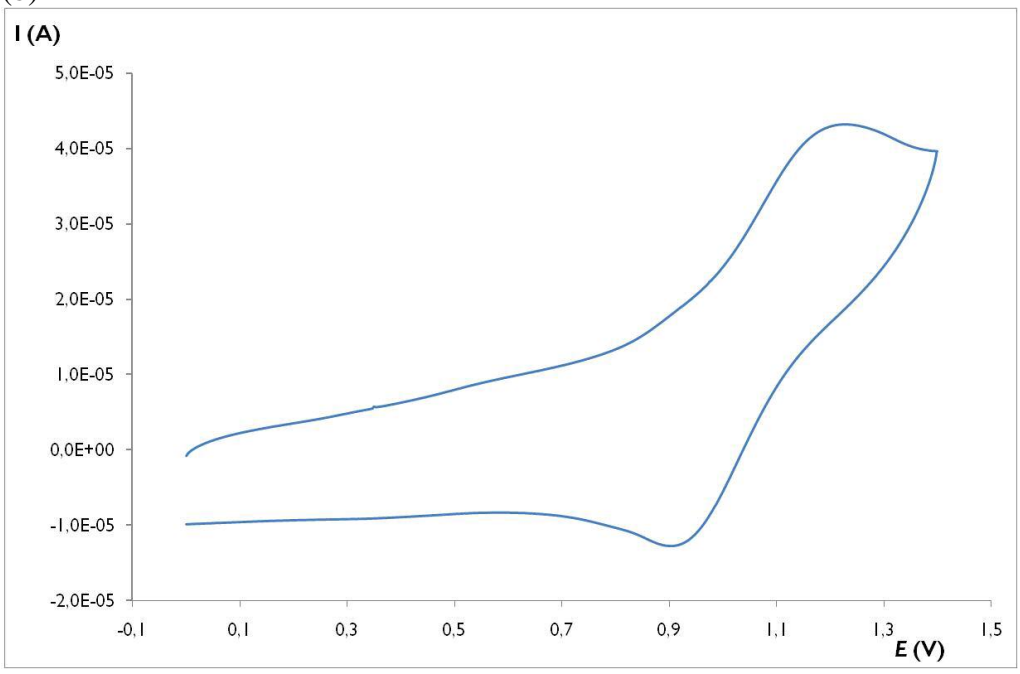

Figure S9. Cyclic Voltammetry (CH_2Cl_2 + 0,1M TBAP, 100 mV/s) of complexes containing the **L2** ligand. (a) [Ru^{II}Cl(L2)(bpy)](BF_4), **5** (b) [Ru^{II}Cl(L2)(dppe)](BF_4)**, 6**.

(a)

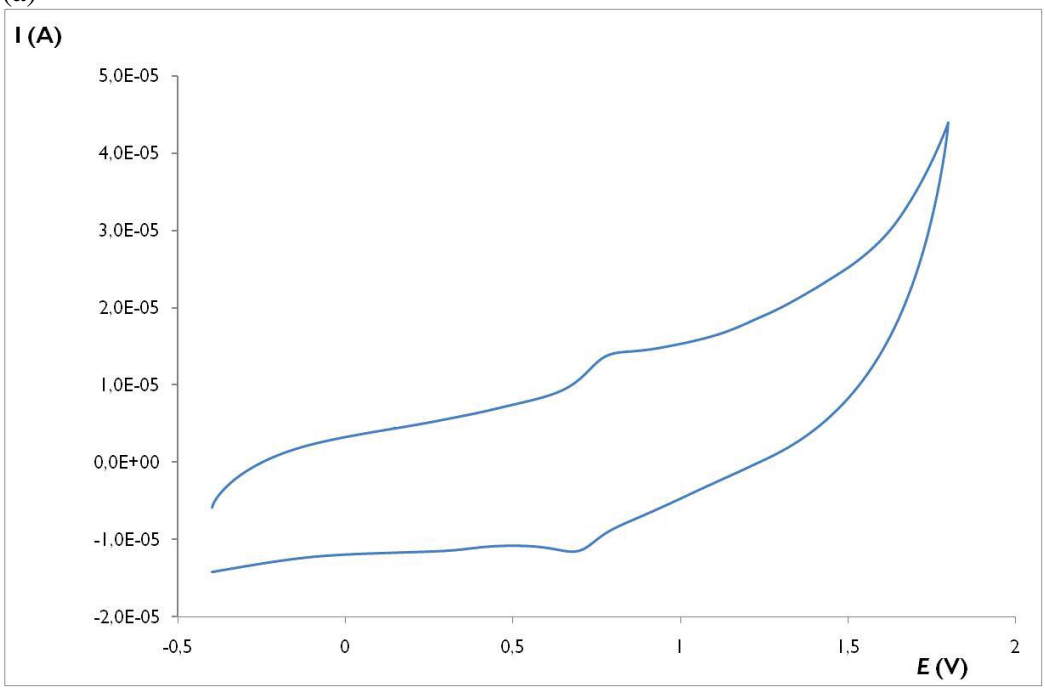

(b)